Annals of Biology **42** (1) : 80-86, 2026 **http://agribioj.com** **Impact Score : 0.32 (Scopus)**

Response Surface Approach for Acid Red 66 Dye Removal Using Alkali Treated Rice Husk

TAMANNA KUMARI, LAKHVINDER SINGH* AND PALLAVI PUNIA[1]

Department of Environmental Science & Engineering, Guru Jambheshwar University of Science & Technology, Hisar-125 001 (Haryana), India
**(e-mail: lakhvinder16@gmail.com; Mobile: 94668 85605)*

(Received: August 9, 2025; Accepted: September 17, 2025)

ABSTRACT

Rice husk, a promising agriculture-based biosorbent, was used for the removal of Acid Red 66 dye in the present study. Alkali-treated rice husk was used to adsorb said dye from simulated aquatic solution. SEM and FTIR were used to evaluate the chemical makeup of rice husk which showed positive changes in chemical composition of alkali-treated rice husk. The primary components of the materials under analysis were lignin, cellulose and hemicellulose. Standard commutative models for the response surfaces and percentage adsorption were obtained by evaluating the adsorbents by applying Box-Behnken designs with independent variables which included pH, concentration of dye and different adsorbent dose. Rice husk showed a very high percentage of adsorption of Acid Red 66 dye (95.45%). Regeneration study showed reusability and future prospective of alkali-treated rice husk for the treatment of dye containing waste waters.

Key words: Agricultural waste, rice husk, adsorption, Acid Red 66, SEM

INTRODUCTION

Extensive research has been conducted to create a circular economy in response to the growing need for sustainable and efficient solutions to overcome the contamination of aquatic environments by high density metals and dyes (Oulkhir *et al.,* 2023). Because these are abundant and toxin free bio-based materials made from living things have gained a huge amount of attention (Mojiri *et al.,* 2022). Due to discharge of textile pollutant like different synthetic and natural dyes into aquatic body, the enormous growth of the textile industries has resulted in a considerable amount of water pollution**.** Industrial effluents include a huge quantity of dyes, when discharged into surrounding atmosphere without adequate treatment, pollute water. In the dying processing industry, Acid Red 66 is a common acidic negative charged azo molecule. Because of dyes' intricate chemical structures, which include azo groups (N=N), aromatic rings, and auxochromes (-OH, SO_3), azo dyes have toxicological characteristics that make them extremely durable and challenging to biodegrade. As a result, their presence even below 1 ppm dissolved in drinking water is extremely noticeable and unpleasant for everyday use. Inhibition of biota, dependently degraded photosynthesis, and decreased solar penetration through water raising the level of toxicity are the disastrous and effects of releasing wastewater with significant dye content into the water without adequate treatment (Allouss *et al.,* 2019). At this stage treatment of gray water released from these industrial units become a crucial need because this waste water is main cause to make the dyes more readily available in different type of water bodies such as river and lakes. Since it causes the dyes to become more readily available in the aquatic environment, it is therefore imperative that aqueous solutions released by the industries may be properly treated. The extreme levels of chemicals, suspended microscopic dust particles, and dangerous substances, unwanted waste waters are those that include dyes. Approximately 10-15% of the dyes generated worldwide are released as waste water. Prime goal of this research work was acid red 66 dye removal, which are widely utilized in the textile sector.

[1]Department of Chemistry, School of Chemical Engineering and Physical Sciences, Lovely Professional University, Phagwara 144 411 (Punjab), India

The European Chemical Agency states that acid red dyes are dangerous for the aquatic environment when they are discharged into aquatic systems. To remove pollutant from different water bodies, many treatment techniques have emerged, including coagulation, flocculation and filtration by using membrane, ozonation, sedimentation, electro-precipitation, and adsorption. There has been a lot of interest in using biogenic materials for environmental purposes. Rice husk is a significant agricultural waste that requires careful handling (Narayanasamy *et al.,* 2022). The primary goal in the present study was to determine application of an inexpensive biosorbent for waste water treatment. Adsorption a surface related technique that effectively removes harmful colors from wastewater through a physical-chemical process.

MATERIALS AND METHODS

Analytical grade NaOH, HCl, commercial dye Acid red 66 of highest purity were obtained. Rice husk was collected from a local village Asthalbhor, Rohtak, India. Rice husk was repeatedly cleaned using distilled water until complete elimination of contaminates. It was dried under sun for 5 days for complete removal of moisture. Thereafter, it was pulverized into fine powder using grinder and sieved (300 mm) to convert into fine particles. The alkali treatment (NaOH) was done to activate surface of rice husk. Rice husk biosorbent was dipped in to NaOH solution having 0.10 mol/L concentration for 24 hours. Distilled water was used to wash rice husk until pH became neutral. It was further dried at 70 °C for 24 hours in a hot air oven to remove moisture. It was stored in air resistant container for additional processing. Fig. 1 shows steps followed for preparation of rice husk biosorbent for dye removal. Analytical grade commercial textile dye Acid red 66 ($C_{22}H_{14}N_4Na_2O_7S_2$) was obtained from standard supplier. Fig. 2 explains structure of Acid red 66 dye.

The image of SEM was formed using the Quanta 250 FTI optical instrument JEOL. It showed morphology of the rice husk biosorbent. Functional groups in adsorbents were identified using FTIR spectrometer, Modal JSM-7610 plus.

The stock solution of Acid Red 66 dye was prepared, and desired dilutions were made from the stock solution. Adsorption studies using different dye concentrations, pH levels, and dosages were performed with Acid Red 66. The original pH measurements from the Acid red 66 solutions were recorded using a pH meter.

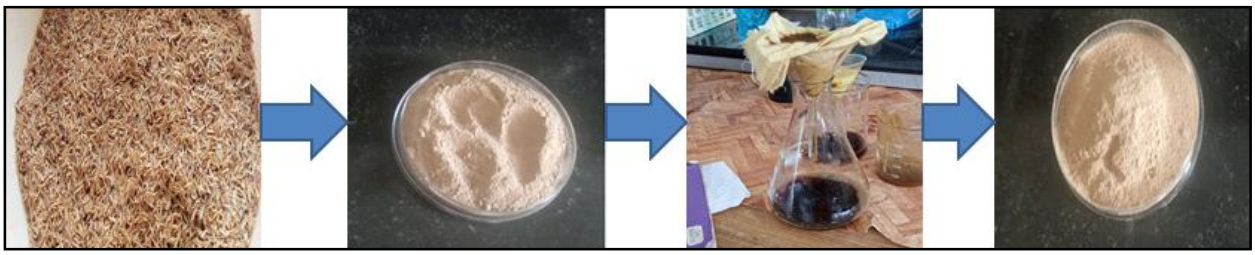

Fig. 1. Preparation of rice husk biosorbent in dye removal process.

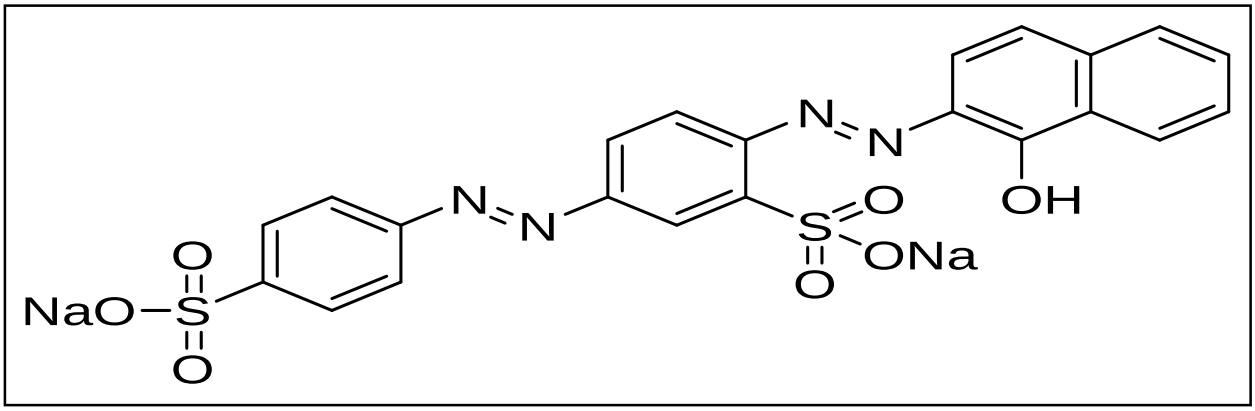

Fig. 2. Acid Red 66 dye structure.

pH was modified using little amounts of concentrated HCl or NaOH.

A UV-1800 SHIMADZU spectrophotometer was used to measure the initial absorbance (Abs^0) of each Acid Red 66 dye sample at 505 nm. Samples were made in conical flasks using 100 mL of each Acid Red 66 solution and the desired concentrations were prepared. Conical flasks were sealed and kept at 30 °C in an incubator shaker for two hours at 120 rpm. For filtration of samples Whatman filter papers were used, and the measurement of absorbance was done at 505 nm. All the experiments were conducted in triplicates.

Table 1 shows independent variable such as pH, dose and concentration in coded variable form. With 17 trials and three duplicates, Box-Behnken Design was applied for experimental finding in Response Surface Methodology (RSM) adsorption assays. Table 2 shows Box-Behnken design model for coded variables representing pH dose concentration. For response surface method (RSM), the adsorption tests used the Box-Behnken experimental design, with 17 trials (in 3 replicates). The factors chosen were: the alkali-treated rice husk biosorbent's pH, Acid Red 66 concentration, and dose.

$$\text{Extent of dye Removal (\%)} = \left(\frac{Ci - Ce}{Ci}\right) \times 100 \ldots \text{Eq. 1}$$

Where, Ci was initial concentration of dye used in experiment and Ce was equilibrium concentration.

Table 1. Formulation of different parameters of pH dose concentration

Independent variable	Level of coded variable (Range)		
	Low (-1)	Center (0)	High (+1)
pH	2	6	10
Dose (g/l)	1	2	3
Concentration (mg/l)	20	35	50

RESULTS AND DISCUSSION

SEM Images were formed on the Quanta 250 FEI optical instrument JEOL. It showed morphology of the rice husk biosorbent. Testing samples were metalized by using gold and resultant images were enlarged at 5000x. By examining in the electron micrographs, the morphologies of the biosorbents were evaluated showing even and smooth texture (Fig. 3). However, alkali treated sample showed surface changes. Following alkali treatment, it displayed the active space. The outer epidermis's fissures and ruptures can be seen. These were enlarged than those who did not receive treatment.

FTIR- Functional groups in adsorbents were identified using FTIR spectroscopy using FTIR Spectrometer spectrum Modal JSM-7610 plus. Peak from 500 - 730 showed halogen compound (C-CI) stretching. Peaks at 897 showed aromatic compound. Peak at 1027 to 1037 showed C-O stretching lingo cellulosic

Table 2. Box-Behnken design matrix for coded variables showing actual and predicted value

Experiments	Parameter 1	Parameter 2	Parameter3	Response 1	
	A: pH	B: Dose (g/l)	C: Concentration (mg/l)	R1 Actual value (Dye removal %)	Predicted value
1	-1	+1	0	95.45	95.89
2	0	0	0	87.82	86.96
3	+1	0	+1	85.80	86.32
4	0	0	0	87.83	86.96
5	0	-1	+1	82.25	82.17
6	+1	0	-1	86.85	86.90
7	-1	-1	0	89.87	90.00
8	-1	0	-1	94.73	94.21
9	+1	-1	0	87.00	86.56
10	0	0	0	87.85	86.96
11	-1	0	+1	92.22	92.17
12	0	+1	+1	88.94	88.55
13	0	-1	-1	86.73	87.12
14	+1	+1	0	86.28	86.15
15	0	+1	-1	86.15	86.23
16	0	0	0	85.51	86.96
17	0	0	0	85.81	86.96

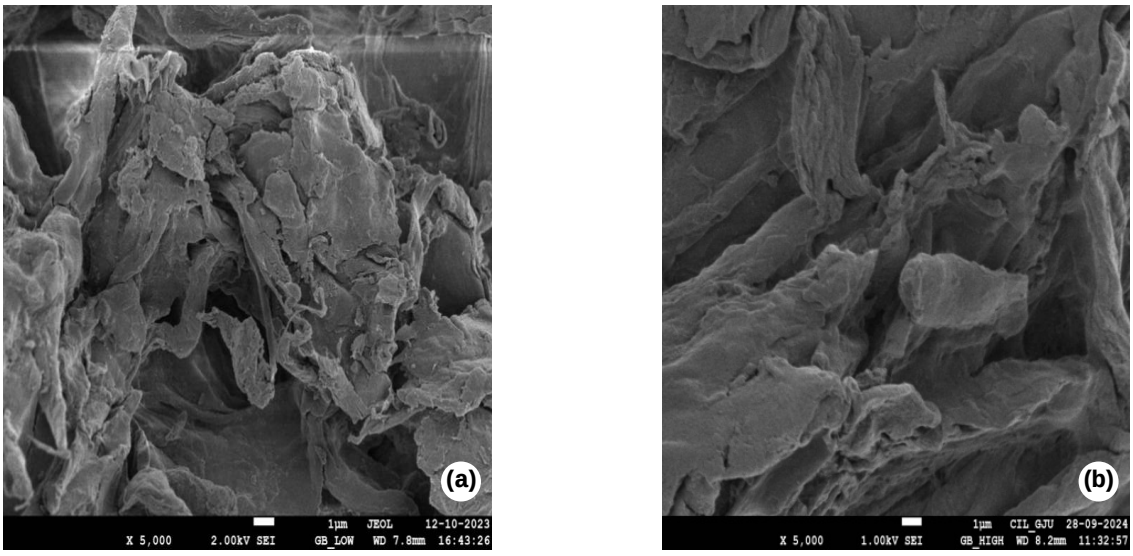

Fig. 3. SEM images of (a) alkali treated rice husk before dye removal (b) after dye removal.

material. Peak at 1110.7 showed COOH stretching. Carboxylic group Peak at 1162 .45 showed COOH stretching and peak at 1500 to 1600 showed presence of lignin. Peak at 2890 to 2930 showed C-H stretching. Peak at 3390 to 3334 showed OH stretching. Major function groups in alkali treated rice husks both prior and after dye removal are shown in Fig. 4.

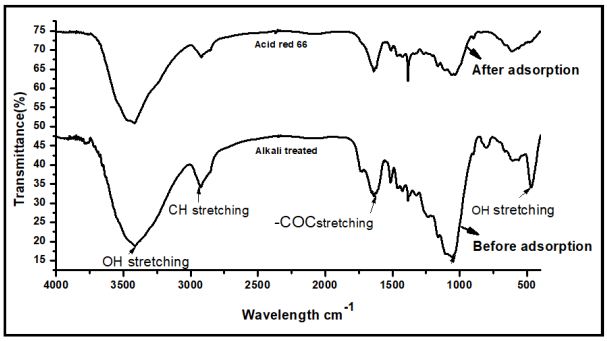

Fig. 4. Peaks in FTIR of rice husk before and after Acid Red 66 dye removal.

To determine the lambda max, Acid red dye solution's wave length was measured using a UV-visible spectrophotometer from 330 to 1000 nm (Boxi and De, 2020). Experimental design was done in pH range from 2 to 10. Biosorbent dose lies between 1 to 3 g/L. Dye concentration lied between 20 to 50 mg/L.

$$\text{Removal \%} = 86.96 - 3.29A + 1.37B - 0.6563C - 1.58AB + 0.3650AC + 1.82BC + 3.28A^2 - 0.5983B^2 - 0.3482C^2 \quad \text{... Eq. 2}$$

Model fitness is shown by ANOVA finding (Table 3). The real experimental values were near to the predicted value as shown in Table 2 which indicated that this modal supported our research finding. ANOVA (Analysis of variance) was used to assess validity as well as statistical significance (95% confidence interval) of constructed models, and coefficient of determination. R^2 and modified R^2 were applied for quality assessment.

Value of Predicted R^2 was 0.8394 which was very close to the Adjusted R^2 (0.9124). Very less difference was seen here (0.2). Adequate Precision was applied to measure signal to noise ratio. A higher ratio more than four was more suitable. 17.9038 ratios showed an acceptable signal. For navigation of design space this concept can be used. Coefficient of determination and coefficient of variation, two goodness-of-fit metrics, were used to assess the quadratic model. With R^2-values of about 0.96, the two models had a decent quadratic fit. The ability of the produced models to forecast the Acid red 66 dye removal efficiencies for any combination of CF parameter within the experimental conditions were indicated by a high R^2-value (higher than 0.75). Additionally, the models' capacity to adequately characterize the adsorption process performance within the specified range of the operational parameters was demonstrated by the closely high adjusted R^2 values. Additionally, the models' capacity to adequately characterize the rice husk process performance within the specified range of the operational parameters was demonstrated by the closely high adjusted R^2 values. Most of the

Table 3. ANOVA findings for quadratic models that were created for Acid red 66 dye, BBD removal efficiencies

Source	Sum of squares	df	Mean square	F-value	p-value	
Model	175.18	9	19.46	19.61	0.0004	Significant
A-pH	86.59	1	86.59	87.26	< 0.0001	
B-Dose	15.04	1	15.04	15.16	0.0059	
C-concentration	3.42	1	3.42	3.45	0.1058	
AB	9.92	1	9.92	10.00	0.0159	
AC	0.5476	1	0.5476	0.5518	0.4818	
BC	13.21	1	13.21	13.31	0.0082	
A^2	45.51	1	45.51	45.86	0.0003	
B^2	1.51	1	1.51	1.53	0.2565	
C^2	0.5004	1	0.5004	0.5043	0.5006	
Residual	6.95	7	0.9924			
Lack of Fit	1.25	3	0.4168	0.2927	0.8297	Not significant
Pure Error	5.70	4	1.42			
C or Total	182.13	16				
Std. Dev.	0.9989	R^2		0.9617		
Mean	88.06	Adjusted R^2	0.9124			
C.V. (%)	1.13	Predicted R^2	0.8394			
		Adeq. Precision		17.9038		

input variables exhibited strong correlations with the models' outputs, as indicated by the narrow range of the R^2 and modified R^2 values. As a result, no independent variables could be ruled out of the study.

Graph shown in Fig. 5A represents pH of dye solution's impact on removal. Mechanisms of adsorption process are affected by pH (AlGhouti and Al-Absi, 2020). Medium pH significantly affected process of adsorption. Maximum adsorption capability of adsorbent was observed at lower pH values. It was demonstrated that between pH 2 and pH 10, Acid Red 66 was absorbed adequately. Maximum removal of 95.45 % was observed at pH 2. When the pH was basic or acidic, hydrogen bonding and electrostatic interaction were suggested as primary adsorption processes (Borsagli and Borsagli, 2019).

Graph in Fig. 5B shows relationship between concentration of dye and dose of adsorbent. As adsorbent dose increased from 1 to 3 g/L dye removal also increased. 95.45% removal was recorded. The rate was significantly impacted by the adsorbent's dose rate of dye removal and was a crucial component of adsorption process to investigate effects of dose of adsorbent on Acid Red 66. Higher removal efficiency resulted from an increase in the adsorbent surface's active site count as the dose of adsorbent rised. As the adsorbent dose for Acid Red 66 dyes increased, the adsorption capability of the adsorbents diminished (Islam *et al.,* 2019).

Graph in Fig. 5C shows effect of dye concentration. When original dye concentrations were raised from 10 to 50 ppm, the percentage of dye removal often decreased, indicating that there were fewer sites available

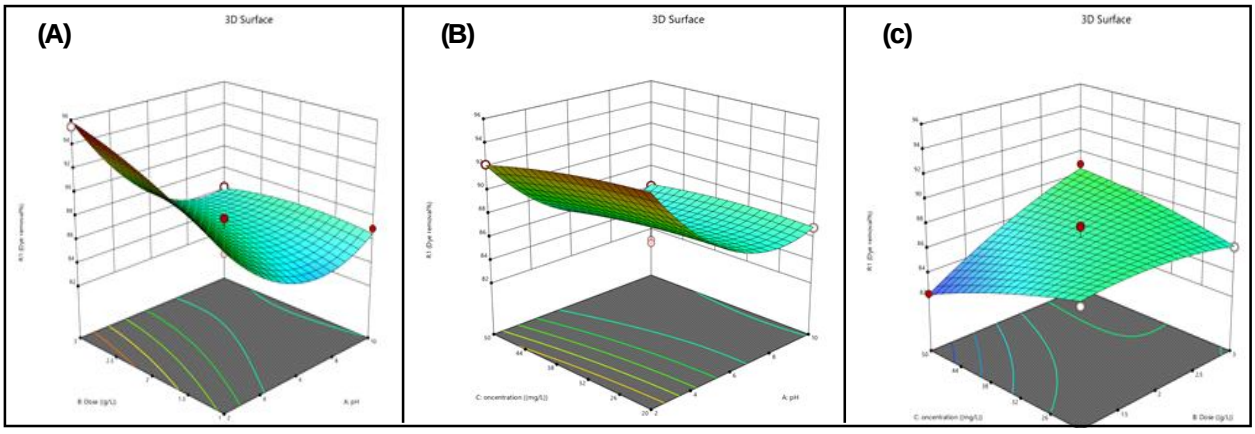

Fig. 5. 3D surface plots of Box-Behnken response surface design showing effect of relationship between (A) Dose and pH; (B) Concentration and pH and (C) Concentration and dose.

for adsorption surface, initial adsorbate concentration, and adsorption site availability are the primary motivating factors for overcoming the adsorbent's transfer of mass barrier in between the bulk solution as well as the adsorbent. The adsorption became prominent at initial lesser concentration of dye because of large number of sites. However, because of the limited active space, the impact grew more noticeable when the dye concentration was increased initially leading to a decrease in dye clearance percentages. As dye concentration started to rise from 20 to 35 ppm the alkali-treated rice husk's enhanced adsorption capacity dramatically from 86.73 to 95.45%.

According to Langumir isotherm model adsorption is a rigorous monolayer process that occurs on adsorbent surfaces that are uniformly coated with a small quantity of active sites. The Acid Red 66 dye range laid between 20 to 50 mg/l, pH value 2, adsorbent dose 3 g/l and 120 min contact time period taken as target (Fig. 6). Langumir and Frendulich adsorption models of isotherms were used to find out behaviour of adsorption and to investigate interaction of Acid Red 66 dye on alkali treated rice husk surface.

Linear and mathematical forms are described in Equations 3 and 4.

$$qe = \frac{qmaxKLCe}{1 + KLCe} \quad \text{...Eq. 3}$$

$$\frac{1}{qe} = \frac{1}{qmax} + \frac{1}{qmKLCe} \quad \text{...Eq. 4}$$

Where, K_L represented Langumir constant, (L/mg), Qmax denoted maximum capacity for adsorption (mg/g), qe denoted equilibrium capacity. Ci and Ce represented initial concentration and equilibrium adsorbate concentration (mg/1). According to Frendulich isotherm process of adsorption occured on heterogeneous adsorbent's material surface, as a result adsorption process took place on multi layers of adsorbent. Liner form and empirical formula of Frendulich isotherm model were represented by Equations 5 and 6.

$$qe = fK_fCe \quad \text{...Eq. 5}$$

$$\log qe = \log k_f + \frac{1}{n} \log c_e \quad \text{...Eq. 6}$$

Where, the Frendulich constant, or K_f, was the adsorption coefficient. Adsorption intensity was denoted by 1/n. Isotherm types were also denoted by using value of 1/n. If the value was more than zero, it was good. As shown in Table 4, R^2 value (0.9623) of Frendulich adsorption isotherm was high as compared to Langmuir

Table 4. Isotherm parameters for the adsorption of Acid Red 66 dye using alkali treated rice husk

Isotherm models	Parameters	Value	Standard error
Langmuir	Intercept	0.0099	1.99162
	Slope	0.0025	3.26488
	Q_{max} (mg/g)	101.0101	
	K_L (l/mg)	3.96	
	R_L	0.201613	
	R^2	0.9044	
Frendulich	Intercept	1.9119	0.0033
	Slope	0.1331	0.01076
	1/n (l/mg)	0.13	
	K_f (mg/g)	81.63568	
	R^2	0.9623	

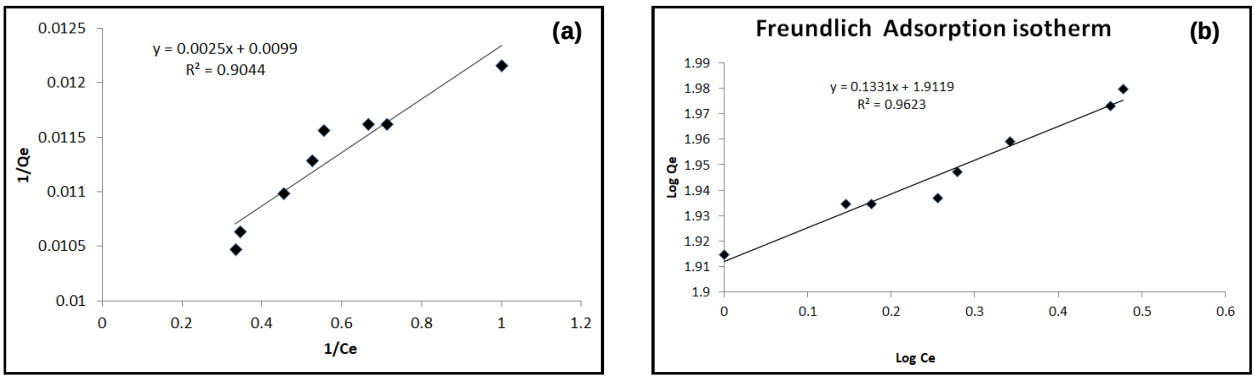

Fig. 6. (a) Langmuir isotherm and (b) Frendulich isotherm for adsorption of Acid Red 66 dye on alkali treated rice husk.

isotherm model (R^2 of 9044). Frendulich isotherm stated that adsorption of Acid Red 66 dye on active site of alkali-treated rice husk was formulated to heterogeneous multilayer interaction (Lin *et al.,* 2020). K_f value was very good (81.63) showing a very high adsorption capacity of alkali treated rice husk (Sharma *et al.,* 2025).

CONCLUSION

Efficacy of removing dye by rice husk after alkali treatment was shown in this investigation using the same dye, Acid Red 66, which was used as a standard dye for adsorption study. Exposure to alkaline chemical provided a basic path to change the morphology of the biosorbent to eliminate cationic species. Adsorption of Acid Red 66 was effectively done in this experiment setup with over 95% adsorption in two hours of contact time. During the study, the adsorption of Acid Red 66 was successfully completed. The Box-Behnken designs of rice husk biosorbent showed that these were versatile over a wide pH range and effectively employed quadratic computed model to explain adsorption study regarding dosage, revelling solution pH and dye concentration.

ACKNOWLEDGEMENT

The authors are thankful to the Department of Environmental Science and Engineering, Guru Jambheshwar University of Science & Technology, Hisar, Haryana, India for providing necessary facilities for conducting this research work.

REFERENCES

AlGhouti, M. A. and Al-Absi, R. S. (2020). Mechanistic understanding of the adsorption and thermodynamic aspects of cationic methylene blue dye onto cellulosic olive stones biomass from wastewater. *Sci. Rep.* **10**: 1-18.

Allouss, D., Essamlali, Y., Amadine, O., Chakir, A. and Zahouily, M. (2019). Response surface methodology for optimization of methylene blue adsorption onto carboxy methyl cellulose-based hydrogel beads: Adsorption kinetics, isotherm, thermodynamics and reusability studies. *RSC Adv*. **9**: 37858-37869.

Borsagli, F. G. L. M. and Borsagli, A. (2019). Chemically modified chitosan bio-sorbents for the competitive complexation of heavy metals ions: A potential model for the treatment of wastewaters and industrial spills. *J. Polym. Environ.* **27**: 1542-1556.

Boxi, S. S. and De, A. (2020). Application of Cu impregnated TiO_2 as a heterogeneous nano catalyst for the production of biodiesel from palm oil. *Fuel.* **265**, 117019. doi: *https://doi.org/10.1016/j.fuel.2020.117019.*

Islam, M. A., Ali, I., Karim, S. A. Firoz, M. S. H., Chowdhury, A. N., Morton, D. W. and Angove, M. J. (2019). Removal of dye from polluted water using novel nano manganese oxide-based materials, J. *Water Process Eng.* **32**: 100911. doi: *https://doi.org/10.1016/j.jwpe.2019.100911.*

Lin, R., Liang, Z., Yang, C., Zhao, Z. and Cui, F. (2020). Selective adsorption of organic pigments on inorganically modified mesoporous biochar and its mechanism based on molecular structure. *J. Colloid Interface Sci.* **573**: 21-30.

Mojiri, A., Zhou, J. L., Nazari, M., Rezania, S., Farraji, H. and Vakili, M. (2022). Biochar enhanced the performance of microalgae/bacteria consortium for insecticides removal from synthetic wastewater. *Process Saf. Environ. Protect.* **157**: 284-296.

Narayanasamy, S., Sundaram, V., Sundaram, T. and Vo, D. V. N. (2022). Biosorptive ascendency of plant-based biosorbents in removing hexavalent chromium from aqueous solutions–Insights into isotherm and kinetic studies. *Environ. Res.* **210**: 112902. doi: *https://doi.org/10.1016/j.jece.2023.110419.*

Oulkhir, A., Lyamlouli, K., Danouche, M. and Benhida, R. (2023). Biosorption of a cationic dye using raw and functionalized *Chenopodium quinoa* pericarp biomass after saponin glycosides extraction. *J. Environ. Chem. Eng.* **11**: 110419. doi: *https://doi.org/10.1016/j.envpol.2025.125842.*

Sharma, V., Solanki, A., Sharma, P. and Kumar, D. (2025). Efficient removal of Lambda-cyhalothrin from simulated water using co-composted-biochar: A modern day substituent of conventional bioadsorbent. *Environ. Poll.* **369**: 125842. doi: *https://doi.org/10.1016/j.envpol.2025.125842*.